Appendix N

DEVELOPMENT OF CLIMATE DATA SETS

TABLE OF CONTENTS

LIST OF TABLES

LIST OF FIGURES

1.0 INTRODUCTION

This document describes the work done to develop the climate datasets used in the Phase 2 Project.

A climate layer consisting of a 500 m by 500 m grid was developed by the University of Lethbridge, Agriculture and Agri-Food Canada and Environment Canada for use in water demand modelling and other applications. Estimates of daily maximum and minimum temperature, as well as daily precipitation, have been derived for the mid-point of each climate grid cell using observed data, for the period 1961 – 2006. For the purposes of this project the period 1996-2006 was examined in more detail. In addition, 12 data sets consisting of daily temperature and precipitation estimates have been generated for each day going back to 1961 and ahead to 2100. These 12 datasets were derived using 6 different General Circulation Models (GCMs), each running twice. These various climate layers have been used in the Phase 2 project for both water demand modelling and water supply modeling.

The terrain of the Okanagan Basin is diverse and has a strong influence on climate. Water supply and demand models require climate data inputs that reflect this complexity, but climate stations are few and located mainly in the valley bottom. Consequently, spatial interpolation at a suitable scale is required to fill in gaps in temperature and precipitation data. A number of approaches have been used previously to develop models which incorporate spatial correlation and topographic effects on climate data. These include GIDS (Gradient plus Inverse-Distance-Squared), which weights predictions derived from a multiple regression equation with the inverse distance to nearby climate stations within a specified radius (Nalder and Wein, 1998) and PRISM (Parameter-elevation Regressions on Independent Slopes Model) (Daly et al.1994), which takes into account elevation but also topographic facet (aspect). Other approaches include DAYMET (DAilY METeorology) (Thornton et al., 1997), which uses weighted observed climate values within a search radius using a Gaussian filter with a shape parameter and ANUSPLIN (Australian National University SPLINe) (Hutchinson 1995, 1999) which

uses a thin plate spline algorithm to fit a smooth surface through data values. Each of these methods has shortcomings in mountainous regions where terrain variations have a substantial effect on local climate.

To account for temperature inversions (warm air overlying cold air), two atmospheric layer models have been used. For example, Daly et al. (2003) divided meteorological point data into two sets and used a standard inversion height (based on radiosonde data) and predefined inversion locations were specified.

In addition to terrain, large water bodies can also influence climate patterns significantly. Perry and Hollins (2005) used the surface area of water within a 5 km radius of each climate station as a predictive variable for gridding monthly climate surfaces for the United Kingdom. Incorporating the area of surface water around each climate station in the regression-interpolation methodology worked well in all seasons, with the exception of the summer months.

In this study, we have created an interactive model for deriving gridded estimates of daily T_{min} (minimum temperature), T_{max} (maximum temperature), and precipitation for the Okanagan Basin (Figure 1.1).

An inverse distance weighting (IDW) interpolation algorithm similar to GIDS was used in conjunction with regional linear and non-linear regression to generate the climate surfaces from weather station data. In addition to latitudinal and elevation influences on temperature and precipitation, temperature inversions are accounted for using a two-layer method and lake effects are modelled by establishing the average long term temperature modification on station T_{max} values.

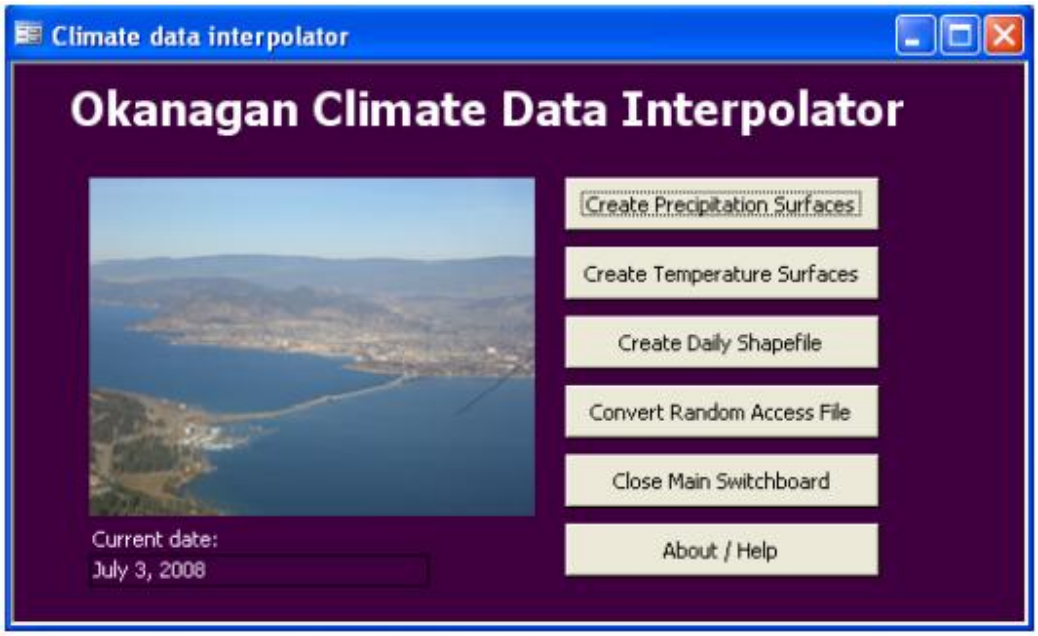

Figure 1.1 Okanagan Climate data interpolator

This study builds on past work that investigated the impacts a warmed climate could have on water resources in the Okanagan Basin (Cohen and Kulkarni, 2001; Neilsen et al., 2001; Cohen et al., 2006; Neilsen et al., 2006). The climate surfaces used in these studies were based on the monthly climate grids produced using PRISM. At a spatial scale of 4 and 1 km, the PRISM grids were too coarse to differentiate valley and mid-slope locations (Neilsen et al., 2001; 2006).

2.0 MATERIALS AND METHODS

2.1 REGIONAL CLIMATE

The Okanagan Basin region has a dry, continental climate due to its location in the rain shadow of the Coast (and Cascade) mountain ranges.

A large proportion of the mean annual precipitation received by the Basin is lost through evaporation and sublimation. Hall et al. (2001) reported that 88% of the mean annual

precipitation is lost through these processes, and other studies have estimated similarly high losses. Basin averages such as those reported by Hall et al. (2001) mask the strong elevational and north-to-south climate gradients that extend up the 160 km valley. The southern extent of the basin is much warmer and drier than the north (Table 2.1). There is an obvious orographic effect as average annual precipitation ranges from just under 300 mm to just over 400 mm south to north in the valley bottom, but up to 770 mm in sub-alpine regions.

Table 2.1 Climate normals in the Okanagan Basin (1971 – 2000)

Station Name	**Elevation (m)**	**Latitude**	**Average Max. Temp. (^oC)**		**Average Min. Temp. (^oC)**		**Average Precipitation (mm)**	
			Jan	Jul	Jan	Jul	Jan	Jul
Osoyoos	297	49^o 01’	1.0	29.2	-5.2	14.1	27.8	24.3
Kelowna A	430	49^o 57’	-0.2	27.6	-7.4	10.7	30.8	36.9
Vernon Coldstream	482	50^o 13’	-1.9	26.6	-8.1	11.6	40.2	40.7
Joe Rich Creek	875	49^o 51’	-1.9	24.3	-10.9	6.3	43.3	55.1
Peachland Brenda Mines	1520	49^o 52’	-4.0	19.2	-10	8.2	75.9	49.1
Vernon Silver Star*	1572	50^o 21’	-4.3	14.9	-9.2	3.2	112.8	93.4

(Online data http://www.climate.weatheroffice.ec.gc.ca/climate_normals/stnselect_e.html, accessed 03/28/2005) * Climate normal from Environment Canada not available. Data derived from observed record for current study.

2.2 CLIMATE DATA

Meteorological data were acquired from the Canadian Daily Climate Data - Temperature and Precipitation CD for Western Canada (Environment Canada, 2000). In total, data from 168 stations (66 within the basin and 102 within approximately 70 km) were extracted from the data CD (Figure 2.1) and used to generate a 47 year meteorological database of daily T_{max}, T_{min}, and precipitation (1960 - 2006). The lack of mid-high elevation meteorological stations in the Okanagan Basin (Table 2.2) necessitated the incorporation of the stations surrounding the Okanagan valley and data from other weather data networks including the BC Environment Snow Pillow stations; BC Ministry

of Transportation Highways Network and the BC Ministry of Forests Fire Weather Network (Figure N.2).

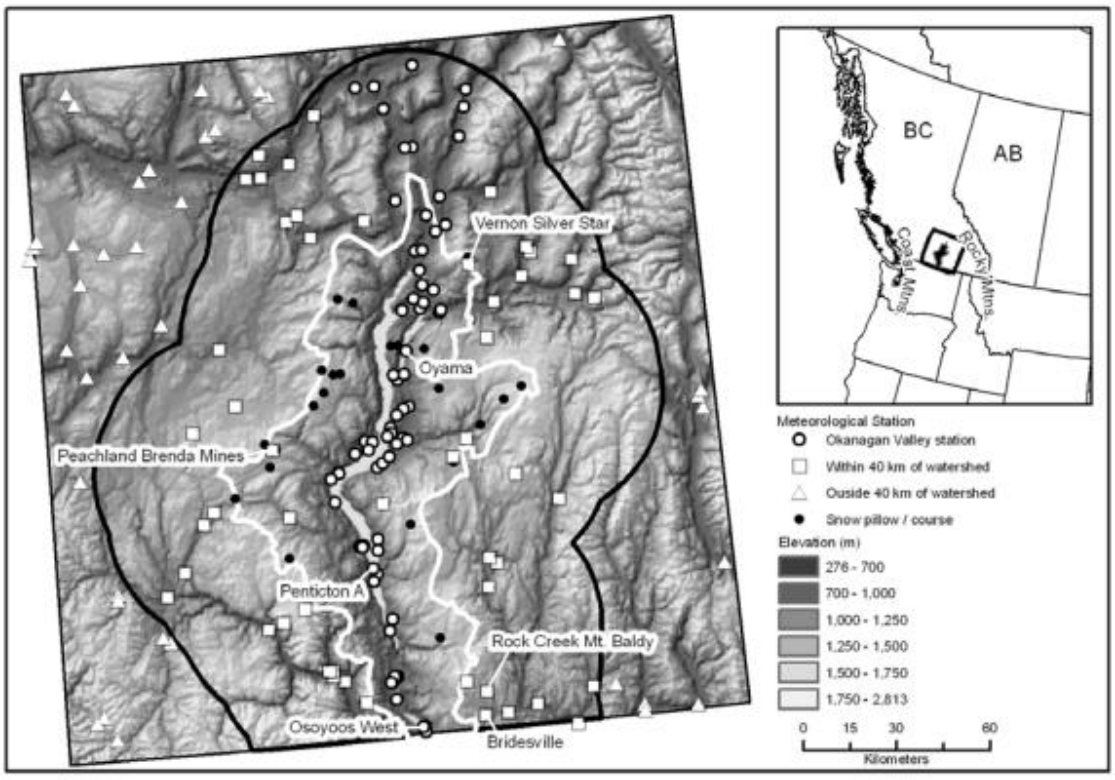

Figure 2.1 Map of the Okanagan Basin map showing the study area and locations of climate stations

Table 2.2 Number of stations reporting on January 1st at low, mid, and high elevation in the Okanagan Basin

Year	< 1000 masl	1000 – 1500 masl	> 1500 masl
1960	18	3	0
1965	19	2	0
1970	20	3	3
1975	26	5	3
1980	26	4	3
1985	30	7	3
1990	28	4	3
1995	35	5	4
2000	30	4	3
2005	23	4	4

2.3 DIGITAL ELEVATION DATA

A digital elevation model (DEM) with a 100-m grid cell size was created as a mosaic from DMTI Spatial's (Markham, Ontario) digital database. A sensitivity analysis of grid cell size on model error indicated that the optimal spatial resolution for the climate interpolation model was 500 m. Thus, to increase computing efficiency and reduce disk storage requirements, while maintaining model integrity, the 100 m DEM was re-sampled to a grid cell size of 500 m using bilinear interpolation.

2.4 MODELLING METHODS

The spatial analysis involves accounting for spatial, elevation, lake effect, temperature inversion, and latitudinal variability in the meteorological data. Interpolation by inverse distance weighting (IDW) was undertaken using the Spatial Analyst feature of ArcGIS (ESRI, Redlands, CA). Model structure and decision-making for temperature grids are outlined in Figure 2.2.

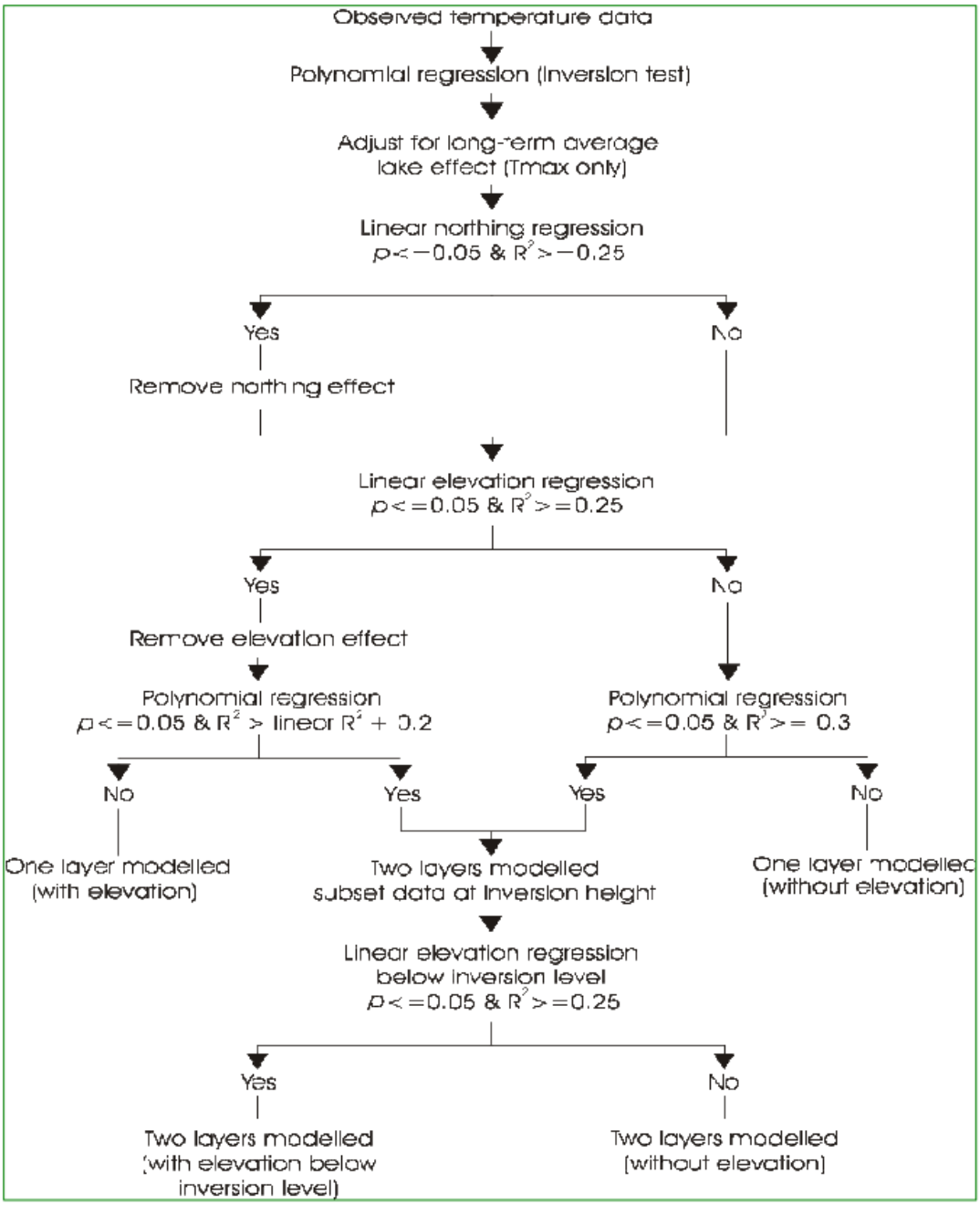

Figure 2.2 Model decision structure for T_{min} and T_{max} inversion and elevation-trend detection.

2.5 HISTORIC TEMPERATURE GRIDS

Daily maximum and minimum temperature grids were created using a series of simple regression analyses according to the logic in Figure 2.2 to remove the effects of elevation, latitude, large lakes and temperature inversions (Neilsen et al., 2010). Daily regression residuals of T_{max} and T_{min} are interpolated using IDW. Following the interpolation, the effect of the explanatory variables (elevation and latitude) is re-introduced to the interpolated residual grid, thereby creating a spatial representation of each variable on a daily basis (Figure 2.3). Interpolating these climate variables after removing the effect of elevation and latitude reduces the spatial bias errors that can occur with simple regression models and incorporates a spatial interpolation component for the unexplained component of the regression models (i.e., residual data values).

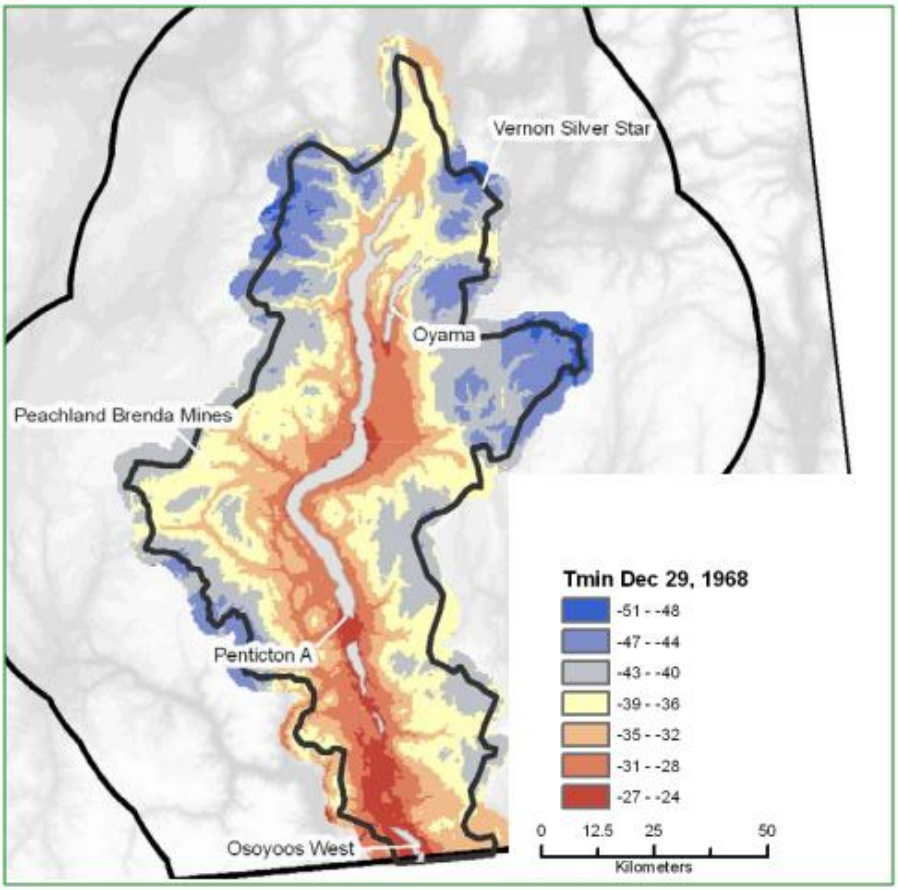

Figure 2.3 Minimum temperatures on the coldest night during the period of record

The elevation regression is applied if the trend is significant ($p \leq 0.05$) and the R^2 value is greater or equal to 0.25. The R^2 cut off was implemented to enhance the ability to detect inversions, and subsequently apply the two-layer model. Instead of extrapolating daily calculated lapse rates the constrained lapse rate approach of Stahl et al. (2006) was applied. Using the constrained approach default lapse rates, averaged by month, were used for grid cells in which the elevation is greater than the highest meteorological station that reported on any given day. The monthly default lapse rates were taken from Stahl et al. (2006) and were calculated using paired stations (Vernon Silver Star Lodge [1572 m] and Vernon Cold Stream Ranch [482 m]).

While the elevation-temperature regressions are calculated using all stations within 40 km of the watershed, the latitude-temperature regression is completed using stations located along the Okanagan valley only. The remaining stations located outside of the 40 km buffer are used to reduce the likelihood that the basin boundary extends beyond all meteorological stations that reported on any given day, thereby minimizing the potential for interpolation artifacts along the watershed boundary.

Prior to the daily regression analysis the T_{max} data are adjusted to remove the average cooling/heating effect of surface water bodies for all stations within 5 km of a water body. In our study area, daily lapse rates and the occurrence of temperature inversions in the Okanagan Valley are strongly affected by Okanagan Lake. T_{min} surfaces did not take lake effects into account because T_{min} temperatures are typically measured around 5:00 am and are a function of local topography (Bolstad et al., 1998; Yoshikado and Kondo, 1989).

Also of particular importance are temperature inversions that typically develop at night during clear sky conditions in mountainous terrain (Whiteman et al., 2004). The model incorporates a two-layer approach in which inversions (either T_{max} or T_{min}) are detected by fitting a second order polynomial to the observed data and comparing best-fit statistics with the linear regression model (Figure 2.4). If an inversion is detected, the observed

temperature data are subset into two groups, including: 1) stations within the mixing layer (i.e., below the inversion), and 2) stations at elevations greater than the inversion height. The mixing height is defined as the elevation at which the derivative of a best-fit second order polynomial is
zero.

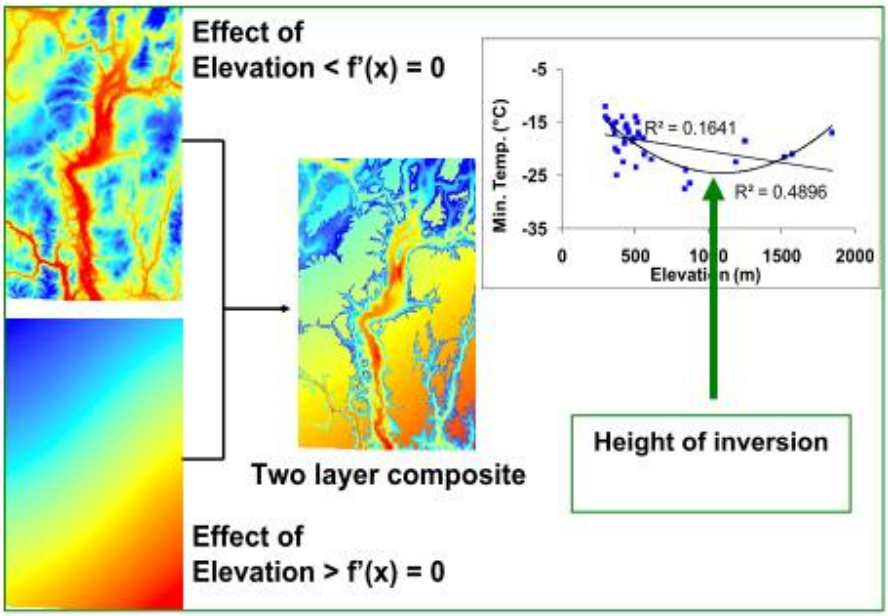

Figure 2.4 Detecting minimum temperature inversions

2.6 HISTORIC PRECIPITATION GRIDS

Daily precipitation grids (Figure 2.5) were created using a similar regression procedure (Neilsen et al., 2010). Prior to the spatial interpolation, the data were de-trended for the north-to-south precipitation gradient and the orographic component of precipitation. Again the north-to-south precipitation gradients were calculated using the Okanagan Valley stations only (Figure 2.1). The precipitation model differs from the temperature model in that the regressions are based on monthly precipitation totals. To derive daily surfaces using monthly elevation-precipitation and latitude-precipitation relationships required the calculation of the percent of monthly precipitation at each station for each day.

Two spatial interpolations are utilized, one for the residual values from the regression analysis and another to interpolate the percent of monthly precipitation on each day. Following the interpolation of daily precipitation percentages and regression model residuals using IDW, Equation 2 is reversed to create daily precipitation grids. In contrast to the one- step regression-interpolation procedures developed by Daly et al. (1994), Thornton (1997), Nalder and Wein (1998), and Hutchinson (1999), the spatial dependences of latitude and elevation were removed before the spatial interpolation because the daily adjustments of each observed precipitation value were based on monthly precipitation totals.

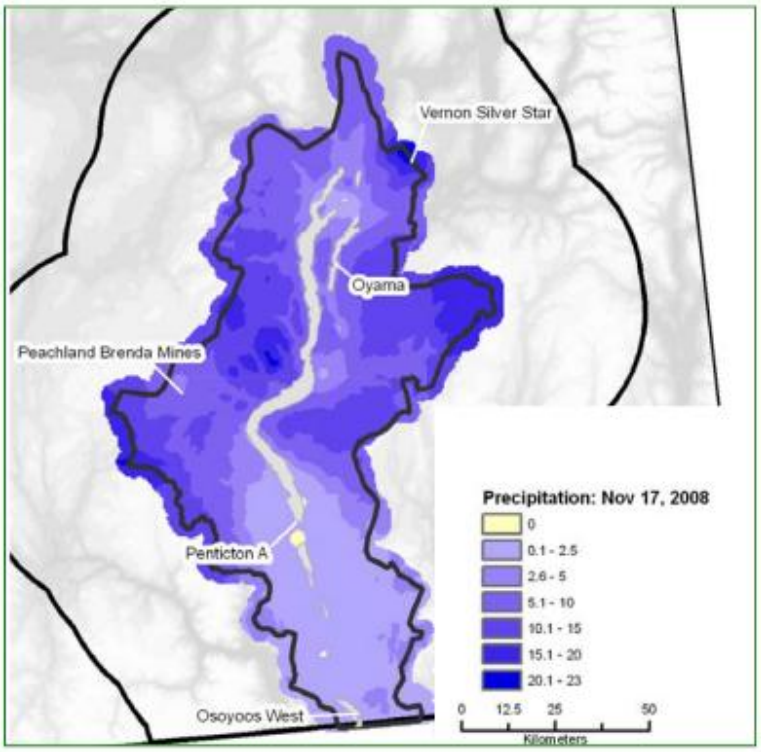

Figure 2.5 Interpolated daily precipitation surface

2.7 FUTURE CLIMATE SURFACES

Future daily temperature and precipitation surfaces were developed using multiple Global Climate Models (GCMs) and 3 IPCC greenhouse gas emissions scenarios (SRES). The six GCMs used were CGCM2, CGCM3, CM2.1, ECHAM5, HadCM3, PCM1. The SRES scenarios included A2 which describes a very heterogeneous world with high population growth, slow economic development and slow technological change; B1 which describes a convergent world, with a global population that peaks in mid-century with rapid changes in economic structures toward a service and information economy and B2 which describes a world with intermediate population and economic growth, emphasizing local solutions to economic, social, and environmental sustainability. No likelihood has been attached to any of the SRES scenarios (IPCC, 2008).

Data were downscaled to 500 x 500m grid cells using TreeGen (Cannon, 2008) a model which combines a synoptic variable classification scheme (Cannon et al., 2002) with a weather generator. In this way, observed synoptic-scale atmospheric predictor variables are related to observed surface weather variables, and then, based on these relationships, realistic series of weather variables are generated from GCM synoptic scale variables. Algorithm details are given in Appendix A of Stahl et al. (2008). Predictors in the classification model were mean sea-level pressure surface air temperature, and surface precipitation data from the US NCEP/NCAR model reanalysis (Kalnay et al., 1996). Daily mean maps from 1948-2006 were obtained for a region covering western North America and the North Pacific Ocean (30°N-70°N; 160°W-110°W). Data were sub-sampled from the 2.5° by 2.5° resolution grid to a 5° by 7.5° grid to facilitate later use with coarser spatial resolution GCM data. Synoptic-scale fields matching those from the NCEP/NCAR Reanalysis were obtained from transient greenhouse gas plus aerosol runs of were CGCM2, CGCM3, CM2.1, ECHAM5, HadCM3, PCM1 for simulated years 1961–2100 with forcing variables from the A2 SRES scenario and one of the B1 or B2 SRES scenarios. Concurrent daily weather conditions in the Okanagan Valley were represented by precipitation amounts, mean temperatures, and diurnal temperature ranges at major surface stations. The "stations" in this case are a subset of points from the gridded climate field. Derived climate normal variables at all points in the basin were

first clustered and were used to split the area into a series of homogeneous climate regions. Finally, the grid points nearest to the cluster centroids served as stations in the downscaling.

3.0 MODEL VALIDATION

3.1 TEMPERATURE GRIDS

For temperature cross-validation, fifty-six sites within the boundary of the Okanagan Basin (Figure 2.1) were withheld from the analysis one station at a time from the meteorological database. The climate surfaces were derived using the remaining stations, and the interpolated data were checked against the observations for the removed stations. The T_{max} and T_{min} mean absolute error (MAE) (average of absolute values of predicted-observed) were determined on a daily basis at each site.

Cross-validation of the predicted temperature surfaces indicated that, the MAE for T_{max} averaged 1.0 (Figure 3.1) for all stations in the Okanagan Basin (Figure 2.1). This is less than errors reported in an earlier study for British Columbia and the Yukon which ranged from 1.22 to 1.99 for different interpolation models (Stahl et al., 2006). Validation errors were affected by elevation, being almost twice as large above 1500 masl than below 500 masl (Figure 3.1a). This is partially the result of there being fewer stations reporting at high elevation, so that the removal of one station for validation purposes has a large effect on the interpolation process. There was some seasonality to the errors which tended to be slightly higher in the winter months, particularly above 1000 masl. In general, errors in predicting T_{max} decreased between 1961 and 2005 (Figure 3.1b). This was associated with an increase in the reporting stations as previously observed by Stahl et al. (2006). For high elevation stations, the temporal decrease in errors was most evident after 1985, and may be due to stations after 1985 being located in the central and northern parts of the basin compared with pre-1982, when high elevation predictions were informed by stations in the western central and southern regions.

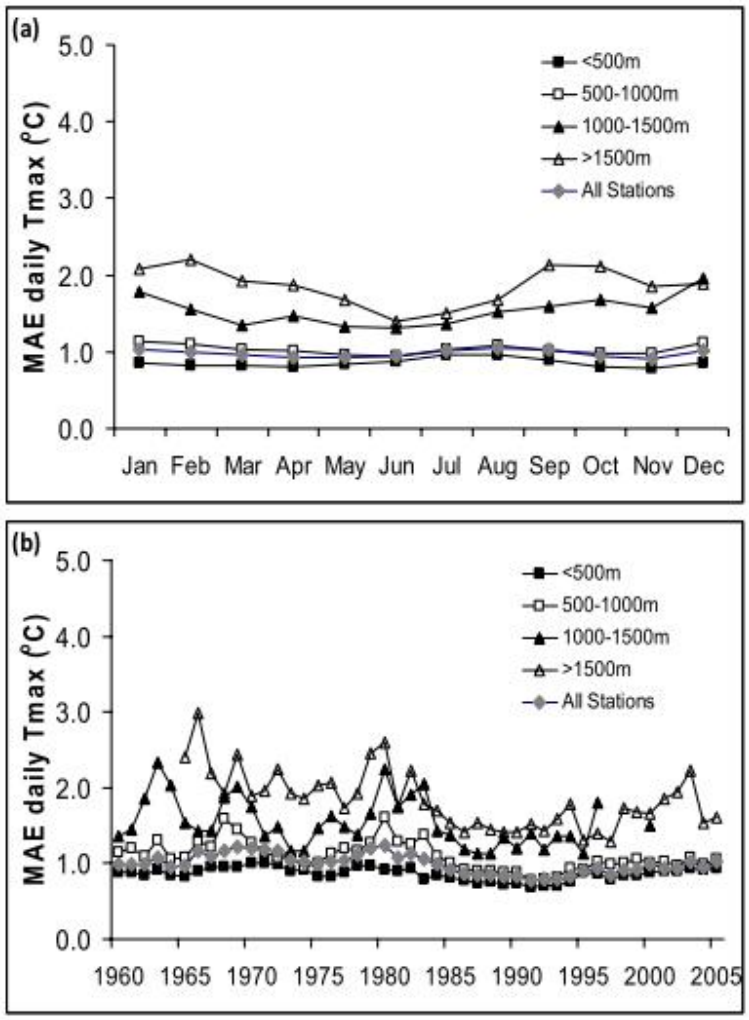

Figure 3.1 Mean Absolute Error for maximum temperatures for each month (a) and each year (b), summarized by elevation band

Mean absolute errors for T_{min} were higher than for T_{max} (Figure 3.2). For all stations, MAE ranged from 1.3 to 1.8 over the year, which is slightly lower than seasonal errors reported previously (Stahl et al., 2006). The effect of elevation on prediction errors was greater for T_{min} (Figure 3.2a) than T_{max} (Figure N.7a). Above 1000 masl, T_{min} cross validation errors ranged from 1.8 to 3.4 over the season, being lowest in spring and fall. Cross validation errors, averaged over all stations, decreased between 1961 and 2005 (Figure 3.2b). As for T_{max}, predictions improved after 1985, likely associated with the location of the higher elevation stations informing the model. Very high errors above

1000 masl in 1982 and 1996 likely resulted from there being only one high elevation station reporting in those years. The model also compares favourably to DAYMET which reported an annual average MAE of 1.8 for daily estimates of T_{max} and 2.0 for T_{min} for a single year for Northwestern United States (Thornton et al, 1997).

For both T_{max} and T_{min}, the model tended to exaggerate temperature extremes, i.e. over-predict high temperatures and under predict low temperatures (data not shown). Predicted minimum temperatures which are lower than observed, would contribute to conservative snow pack melt rates in hydrology models. The relatively small errors for the low elevation stations (Figures 3.1, 3.2) is an indication that the 500 m grid cell size used in this study is an advantage over the 4 km temperature grids that were used for the crop water demand study conducted by Neilsen et al. (2001).

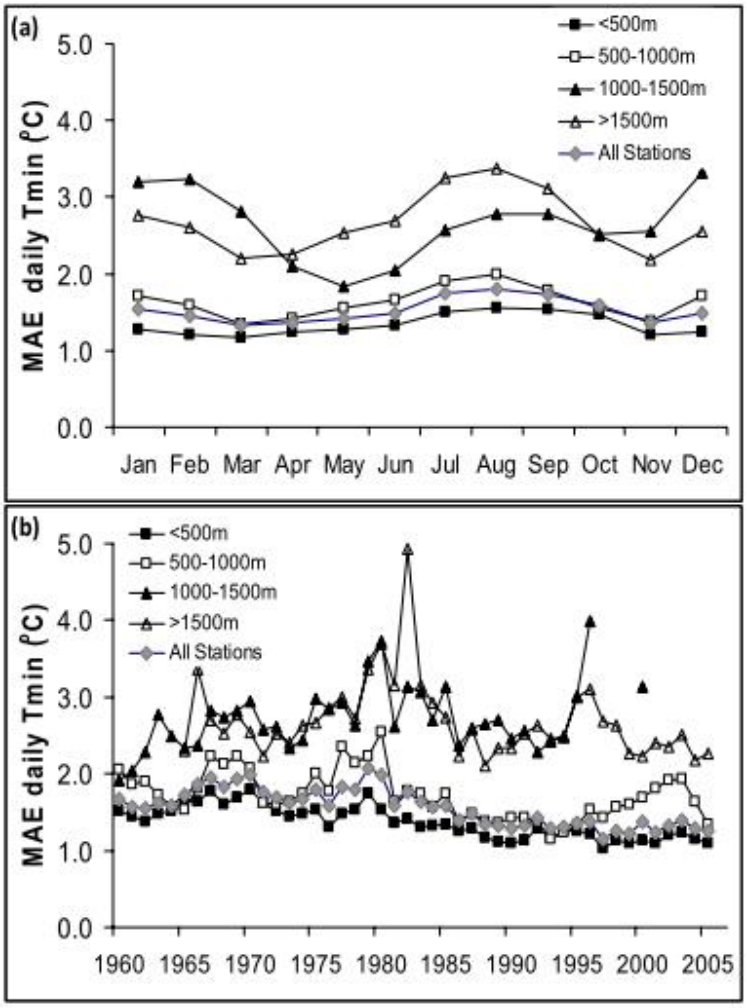

Figure 3.2 Mean Absolute Error for minimum temperatures for each month (a) and each year (b), summarized by elevation band

3.2 PRECIPITATION GRIDS

Cross-validation of the precipitation surfaces was performed for sixty-two sites on a monthly basis because the elevation-regression models were based on monthly precipitation totals. In addition, the daily grids were tested to determine the successful prediction of precipitation occurrence, at all stations, using weather forecast verification techniques for dichotomous (yes/no) forecasts (WWRP/WGNE Joint Working Group on Forecast Verification Research, 2009). Accuracy of predicting days with precipitation (wet days) is defined as: (correctly predicted wet + dry days) / all days) with outcomes

between 0-1.0, and a perfect score being 1.0. Bias of the prediction is defined as (predicted wet days / observed wet days) with outcomes between 0 and ∞, and a perfect score (no bias) being 1.0.

Cross-validation of the monthly precipitation totals indicated that the MAE for precipitation was greatly affected by elevation as errors for stations above 1500 masl were up to six times higher than those for stations below 500 masl (Figure N.9). High elevation MAE was slightly reduced in summer (Figure 3.3a). The large errors at these locations were attributed to the lack of neighboring stations on the same mountain range. For example in 1967, a large error was calculated at Mt. Kobau, which was the only high elevation station reporting within the basin. Similarly, Vernon Silver Star Lodge was the only station above 1500 masl reporting after 2001. The dependency of empirical regression analysis on few high elevation stations is well documented and a common problem in mountainous environments (Running et al., 1987); Daly et al., 1994; Lookingbill and Urban, 2003). Percent errors for each month were calculated and ranged between 3% and 36% (Figure 3.3b) and were more variable at high than low elevation. Over all stations, monthly percent MAE averaged between 10 and 18%. An MAE calculated from simple differences between observed and predicted annual precipitation over all stations was 27 mm with a percentage error of 6.2%. This compares favorably with values for a similar calculation made by Thornton et al., (1997), who reported an MAE of 124 mm, with a percentage error of 19.3% for a single year cross validation study for Daymet. Overall annual MAE calculated from all daily MAE values was 193 , similar in magnitude to the 134 reported by Thornton et al., (1997), but the overall annual bias (observed – predicted daily precipitation) was lower, -3 mm compared with -22 mm.

In addition to verifying precipitation amounts, the ability to properly capture the occurrence of daily precipitation was also tested. Over all stations, accuracy in predicting wet days plus dry days ranged from 0.78 to 0.88 (Figure 3.4). Accuracy improved slightly in the summer months and was highest at low elevation stations (Figure N.10a). The model displays a bias towards over-prediction of days with precipitation of around

1.4 on average (Figure 3.4b). By comparison, DAYMET reported an 83% success rate in predicting precipitation occurrence and a bias of 1.18 for Northwestern United States (Thornton et al, 1997).

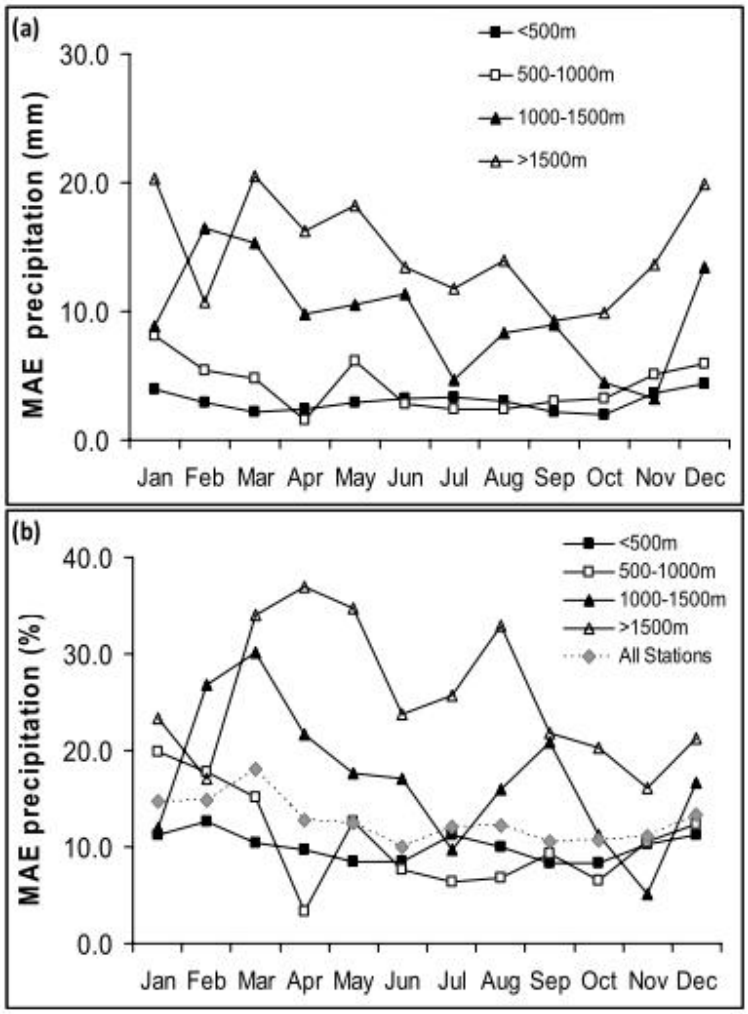

Figure 3.3 Errors in prediction of precipitation for each month (a) MAE (b) percent error, summarized by elevation band

Model bias is likely due to the precipitation algorithm whereby if there is any station at all with rain, then the model would interpolate a very low value for all the stations in a very large area leading to widespread drizzle. An analysis of the amount of precipitation on the incorrectly predicted wet days indicated that over 80% of the days had less than 1

mm of precipitation. To avoid positive bias in the precipitation forecast other models (e.g., DAYMET) have applied a critical value below which precipitation occurrence is negated (Thornton et al., 1997). This technique likely contributed to the lower precipitation bias of the DAYMET model by avoiding erroneous "drizzle" days. While this error would not be considered important for assessing evapo-transpiration, for example, it could be problematic for algorithms that require information on days with and without precipitation (e.g., Bristow-Campbell model for solar radiation) (Bristow and Campbell, 1984).

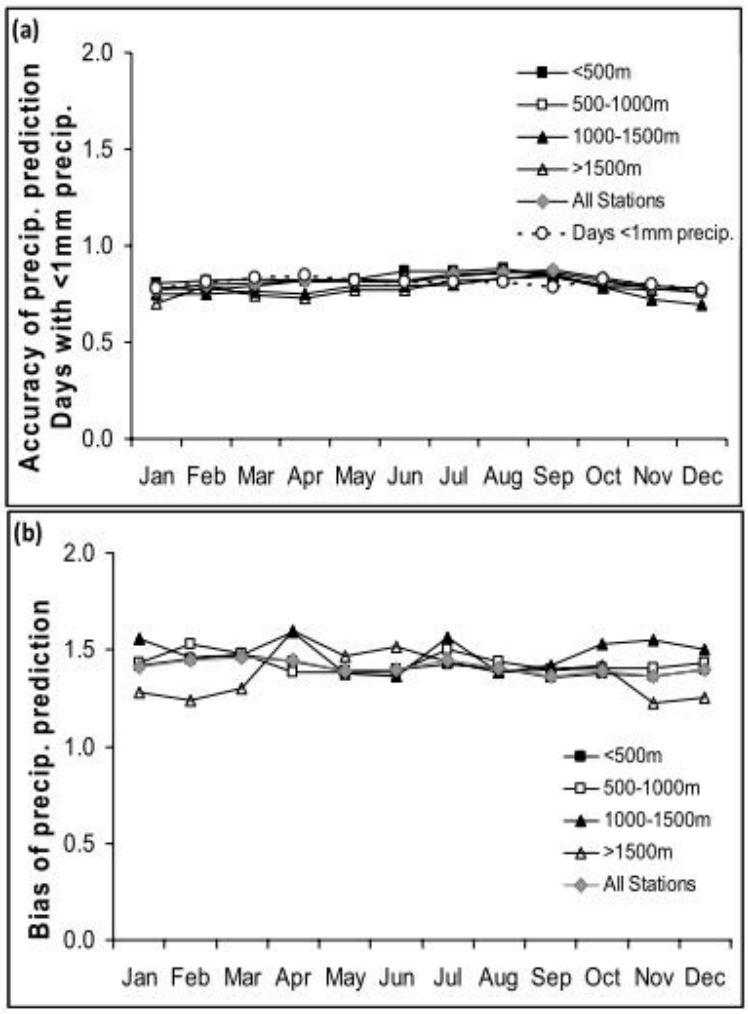

Figure 3.4 Precipitation occurrence statistics: (a) accuracy and the fraction of falsely predicted wet days with precipitation less than 1 mm and (b) bias in the prediction of precipitation occurrence for each month, summarized by elevation band

3.3 FUTURE CLIMATE SURFACES

To assess the TreeGen algorithm's validity, summary statistics and graphical outputs computed from the observations and the models were compared with one another. Mean annual temperature and precipitation were computed for the gridded historic data described above and for each model over the period 1961-2005. Then the corresponding biases (differences between gridded data for observed climate data and simulations downscaled from GCMs) were calculated. To ensure that the models are consistent over time, historic and downscaled data were compared for the period 1961-2000.

3.4 BIAS OF DOWNSCALED REGIONAL TEMPERATURE AND PRECIPITATION MEANS

The plot of mean temperature indicates a shift in observed annual mean temperature beginning in 1986 (Figure 3.5). This shift is also seen in long term weather station data from the Okanagan (data not shown). None of the models exhibited this behavior, resulting in a positive bias prior to that date. A similar shift occurred for annual mean precipitation, with wetter conditions beginning in 1981. Once again the models are unable to discern the change, leading to a negative bias afterwards. Otherwise, the modelled annual means approximate the observed annual means reasonably well in general. The average difference, or bias, of the temperature and precipitation means is shown on Figure 3.6. Relative biases (percentages) are calculated for precipitation. It is apparent that the models are too warm on average, on the order of 0.2°C to 0.5°C. The opposite is true for precipitation, as models predict on average 10% to 16% less precipitation than the observed data. Although no model achieved the lowest absolute bias in both categories, the bar plots suggest that Hadcm3.a2 exhibits best performance. Figure 3.7 displays the corresponding biases for raw GCM outputs. Temperature biases range from -5°C to 3°C, with relative precipitation biases varying from 70% to 170%. Such large biases render raw GCM outputs unreliable. It is clear that downscaling raw GCM outputs via the TreeGen algorithm reduces bias.

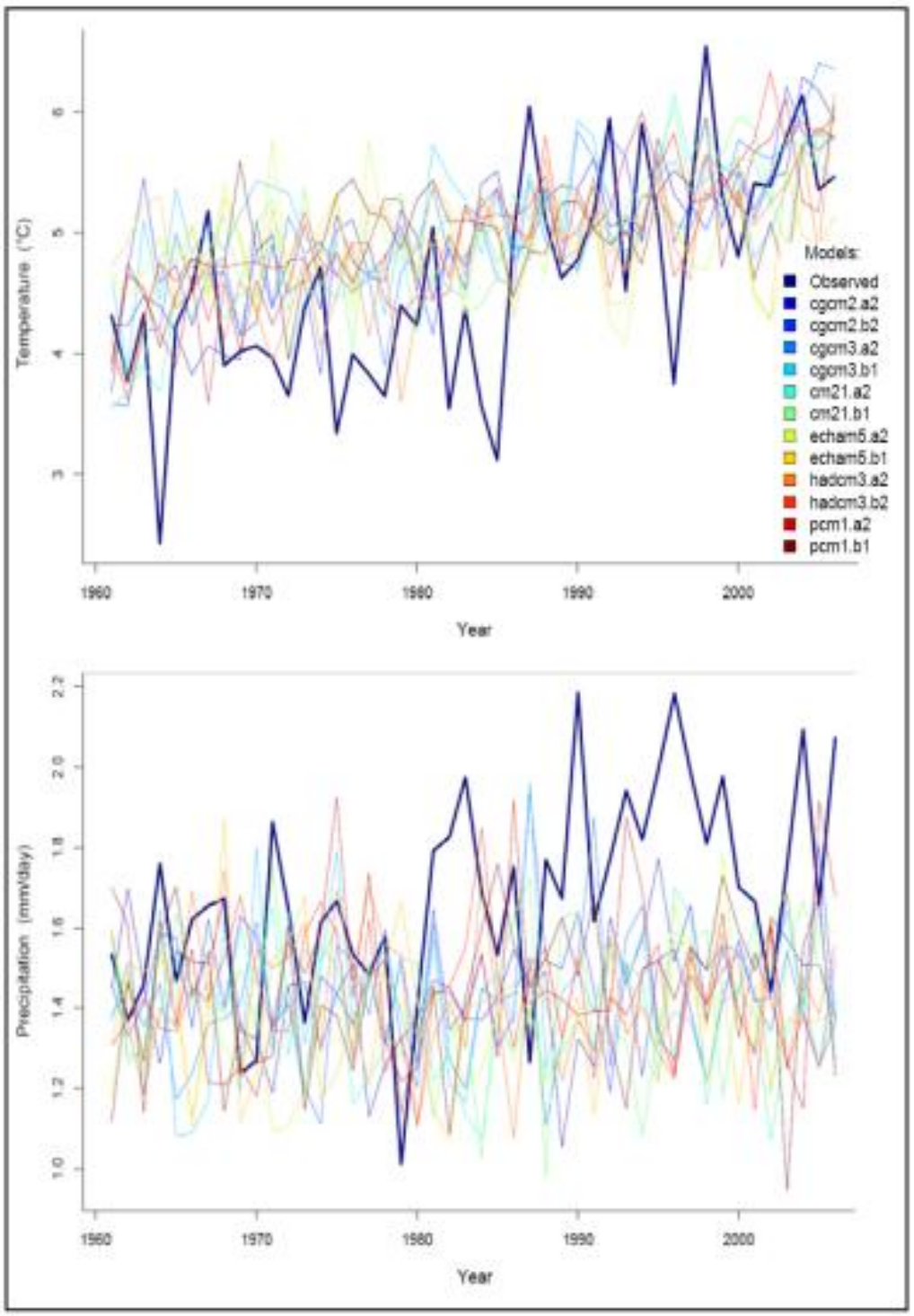

Figure 3.5 Mean annual temperature and precipitation from observations and downscaled GCMs during 1961-2006

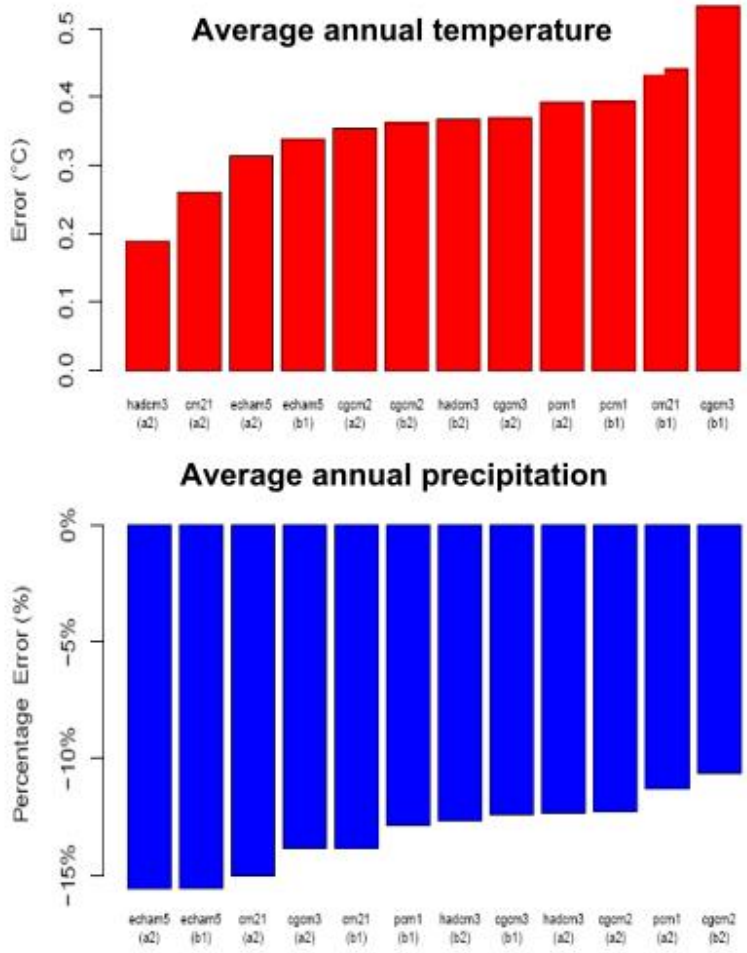

Figure 3.6 Bias in temperature and precipitation projections for a range of downscaled GCMS

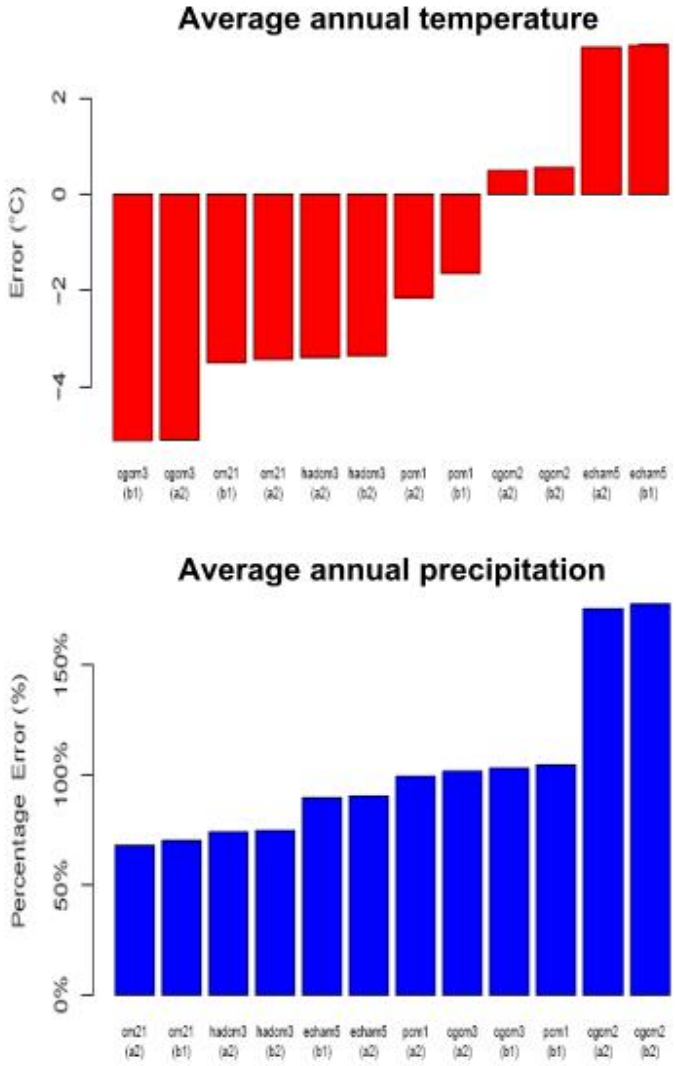

Figure 3.7 Bias in temperature and precipitation projections for a range of raw GCM output

3.5 BIAS CORRECTION

The slightly positive bias in temperature and the larger negative bias in precipitation between downscaled GCM projected and observed climate during the historic period (Figure 3.6) were corrected to allow a better comparison between the effects of climate variation during hydrology model calibration period (1996-2006) and in the future. The monthly mean and variance of T_{mean} and precipitation were calculated for all grid cells over the eleven year period for both the observed and downscaled GCM generated values. For temperature, the bias was calculated by subtracting the observed monthly mean from the downscaled GCM monthly mean. T_{mean} values were used to correct both T_{max} and T_{min} values in order to prevent reversals ($T_{min}>T_{max}$) occurring if corrections were based on bias values derived from T_{max} and T_{min} data. For precipitation the bias was calculated as the percentage difference between the observed and GCM values for each month. The bias correction factors (Table 3.1) were adjusted across monthly boundaries using a smoothing algorithm (Neilsen et al., 2006) to prevent discontinuities between months and then applied to daily data. Bias for temperature was corrected by adding the bias correction factor to downscaled GCM data and for precipitation by multiplying the downscaled GCM data by the bias correction factor.

Table 3.1 Monthly bias correction factors applied to downscaled CGCM2-A2 precipitation and temperature values.

	Jan	Feb	Mar	Apr	May	Jun	Jul	Aug	Sep	Oct	Nov	Dec
Temp (°C)	0.55	-1.08	-0.65	-0.43	-0.02	0.06	0.24	0.43	-0.09	-0.71	-0.14	-0.33
Precip	1.25	0.85	0.96	1.25	1.58	1.66	1.07	0.92	1.50	1.74	1.33	1.06

3.6 TRENDS IN TEMPERATURE OVER TIME

Historic temperature trends in observed values were compared to those derived from the models. Simple linear models were fit to the annual temperature means and annual precipitation means and the slope of the lines were tested for statistical significance. Three methods were used:

Ordinary Least Squares (OLS), robust MM-estimation (MM), and the Sen's method. Standard errors of the estimators were also computed to test the significance of trend. For the Sen's slope, the non-parametric Mann-Kendall statistic was used to test the significance of trend.

For annual mean temperature, the observed trend of about +3.8°C per century is reasonably estimated by all models except echam5.a2 and echam5.b1 (Table 3.2). Except for echam5, the A2 scenario (high emissions) gave rise to slope estimates that are much greater than B1/B2 (low emissions) counterparts. In addition, the three estimators produce estimates that are close approximations of one another for each model. For annual mean precipitation, however, none of the models are able to replicate the observed significant trend of +1.2 mm per century. Nearly all simulations give rise to trend estimates that are close to zero and statistically non-significant, with the directions of trend ambiguous.

Table 3.2 Estimated trend slopes for annual mean temperature and annual mean precipitation for the period 1961-2000. Estimation is conducted by ordinary least squares (OLS), MM-estimation, and Sen's method. Trends significant at the 5% level are in bold

	Temperature Trend (°C/century)			**Precipitation Trend (mm/century**		
	OLS	**MM**	**Sens**	**OLS**	**MM**	**Sens**
Observed	**3.95**	**3.76**	**3.73**	**1.2**	**1.18**	**1.2**
cgcm2.a2	**3.52**	**3.51**	**3.5**	0.11	0.13	0.16
cgcm2.b2	**2.5**	**2.54**	**2.26**	-0.048	-0.07	0.081
cgcm3.a2	**3.18**	**3.05**	**2.82**	0.37	0.34	0.39
cgcm3.b1	**1.83**	**1.7**	**1.63**	1.13	0.11	0.045
cm21.a2	**4.47**	**4.44**	**4.14**	-0.17	-0.19	-0.17
cm21.b1	**2.91**	**2.88**	**2.4**	-0.11	-0.067	-0.2
Echam5.a2	0.55	0.78	1.33	**0.46**	0.4	0.33
Echam5.b1	0.53	0.6	0.37	-0.21	-0.18	-0.14
Hadcm3.a2	**3.07**	**3.05**	**3.09**	-0.27	-0.27	-0.51
Hadcm3.b2	**2.4**	**2.27**	**1.93**	0.086	0.12	0.25
pcm1.a2	**3.78**	**3.7**	**3.59**	0.11	0.055	-0.12
pcm1.b1	**1.98**	**1.91**	**1.85**	**0.5**	**0.55**	**0.66**

4.0 MODEL USES

The Okanagan Climate Data Model (Figure 4.1) drives the supply and demand models used in the Phase 2 project. In conjunction with the Okanagan Water Demand Model (Section 14.0) temperature and precipitation data are used to calculate Penman Monteith reference ET and a range of agro-climatic indices for each climate grid cell (Figure N.14). These are used to derive agricultural and domestic water demand values for the period 1961-2100. In addition, gridded datasets of temperature, precipitation and reference ET have been used to drive the Okanagan Hydrology Model.

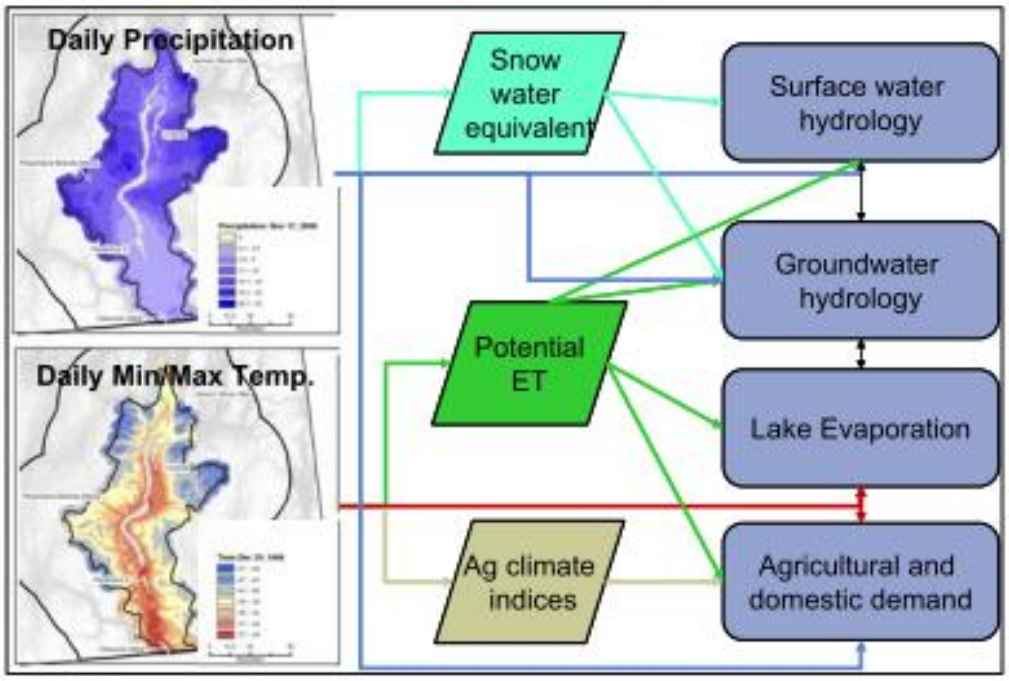

Figure 4.1 Use of gridded climate datasets

5.0 REFERENCES

Bristow, K.L., and G.S. Campbell. 1984. On the relationship between incoming solar radiation and daily maximum and minimum temperature. Agric. For. Meteorol. 31:159–166.

Bolstad, P.V., L. Swift, F. Collins, and J. Regniere (1998), Measured and predicted air temperature at basin to regional scales in the southern Appalachian mountains, *Agr. Forest Meteorol., 91*, 161-176.

Cannon, A.J., and Whitfield, P.H. (2002), Synoptic map classification using recursive partitioning and principle component analysis. *Monthly Weather Rev.* 130:1187-1206.

Cannon, A.J. (2008), Probabilistic multi-site precipitation downscaling by an expanded Bernoulli-gamma density network. *Journal of Hydrometeorology*. http://dx.doi.org/10.1175%2F2008JHM960.1

Cohen, S., and T. Kulkarni (2001), *Water management & climate change in the Okanagan Basin. Environment Canada & University of British Columbia*. Project A206, submitted to the Adaptation Liaison Office, Climate Change Action Fund, Natural Resources Canada, Ottawa, 75 pp.

Cohen S., D. Neilsen, and R. Welbourn (2004), Expanding the dialogue on climate change & water management in the Okanagan Basin, British Columbia, Project A463/433, submitted to the Adaptation Liaison Office, Climate Change Action Fund, Natural Resources Canada, Ottawa, 257 pp.

Cohen, S., D.Neilsen, S. Smith, T. Neale, B. Taylor, M. Barton, W. Merritt, Y. Alila, P. Shepherd, R. McNeill, J. Tansey, J. Carmichael and S. Langsdale (2006), Learning with local help: Expanding the dialogue on climate change and water management in the Okanagan Region, British Columbia, Canada. *Climatic Change 75*:331-358.

Cox, H.J. (1920), Weather conditions and thermal belts in the North Carolina mountain region and their relation to fruit growing, *Ann. Assoc. Am.Geogr., 10*, 57-68.

Daly, C., R.P. Neilson, and D.L. Phillips (1994), A statistical-topographic model for mapping climatological precipitation over mountainous terrain, *J. Appl. Meteorol., 33*, 140-158.

Daly, C., E. H. Helmer, and M. Quinones (2003), Mapping the climate of Puerto Rico, Vieques and Culebra, *Int. J. Clim., 23*, 1359-1381.

Environment Canada (2002), *Canadian daily climate data*, CDCD V1.01, Climate Information Branch, Atmospheric Environmental Service. Ottawa, Ontario, Canada.

Hall, K., J. Stockner, N. Schreier, and R. Bestbier (2001), *Nutrient sources and ecological impacts on Okanagan Lake*. Institute for Resources and Environment, University of British Columbia, Vancouver, British Columbia.

Hutchinson, M.F. (1995), Interpolating mean rainfall using thin plate smoothing splines, *Int. J. GIS, 9*, 385-403.

Hutchinson, M.F. (1999), ANUSPLIN Version 4.0, Australian National University, Canberra, Australia, http://cres.anu.edu.au/software/anusplin.html.

Intergovernmental Panel on Climate Change (IPCC) (2008), Fourth Assessment Report – AR4. http://www.ipcc.ch/ipccreports/ar4-syr.htm

Kalnay, E., M. Kanamitsu, R. Kistler, W. Collins, D. Deaven, L. Gandin, M. Iredell, S. Saha, G. White, J. Woolen, Y. Zhu, M. Chelliah, W. Ebisuzaki, W. Higgins, J. Janowiak, K. C. Mo, C. Lookingbill, T.R., and D.L. Urban (2003), Spatial estimation of air temperature differences for landscape-scale studies in montane environments, *Agr. Forest Meteorol., 114*, 141-151.

Nalder, I.A., and R.W. Wein (1998), Spatial interpolation of climate Normals: test of a new method in the Canadian boreal forest, *Agr. Forest Meteorol., 92*, 211-225.

Neilsen, D., S. Smith, W. Koch., G. Frank, and J. Hall (2001), Impact of climate change on crop water demand and crop suitability in the Okanagan Valley, British Columbia. *Technical Bulletin 01-15*, 32 pp., Pacific Agri-Food Research Centre, Summerland, BC, Canada.

Neilsen, D., S. Smith, G., Frank, W. Koch, Y. Alila, W. Merritt, B. Taylor, M. Barton, J. Hall, and S. Cohen (2006), Potential impacts of climate change on water availability for crops in the Okanagan Basin, British Columbia. *Can. J. Soil Sci. 86*: 909-924

Neilsen, D., G. Duke, W. Taylor, J. Byrne, S. Kienzle, and T. Van der Gulik (2010), Development and verification of daily gridded climate surfaces in the Okanagan Basin of British Columbia. *Can. Water Resources J. 35(2), 131-154*.

Perry, M., and D. Hollins, (2005), The generation of monthly gridded datasets for a range of climatic variables over the UK, *Int. J. Climatol.*, 25, 1041-1054.

Running, S., R. Nemani, and R. Hungerford (1987), Extrapolation of synoptic meteorological data in mountainous terrain and its use for simulating forest evapotranspiration and photosynthesis, *Can. J. Forest Res., 17*, 472-483.

Stahl, K., R. D. Moore, J. A. Floyer, M. G. Asplin, and I. G. McKendry (2006), Comparison of approaches for spatial interpolation of dialy air temperature in a large region with complex topography and highly variable station density, *Ag. Forest Meteorol., 139*, 224-236.

Thornton, P.E., S.W. Running, M.A. White (1997), Generating surfaces of daily meteorological variables over large regions of complex terrain, *J. Hydrol., 190*, 214-251.

Whiteman, C.D., B. Pospichal, S. Eisenbach, P. Weihs, C.B. Clements, R. Steinacker, E. Mursch-Radlgruber, and M. Dorninger (2004), Inversion breakup in small Rocky Mountain and alpine basins, *J. Meteorol., 43*, 1069-1082.

Yoshikado, H., and H. Kondo (1989), Inland penetration of the sea breeze over the suburban area of Tokyo, *Boundary-Layer. Meteorol.*, *48*, 389-407.